Synthesis, Structure, and Nonlinear Optical Properties of Cross-Conjugated Perphenylated iso-Polydiacetylenes

ARTICLE *in* CHEMISTRY - A EUROPEAN JOURNAL · JANUARY 2005

Impact Factor: 5.73 · DOI: 10.1002/chem.200400822

6 AUTHORS, INCLUDING:

Aaron D Slepkov
Trent University
56 PUBLICATIONS **819** CITATIONS
SEE PROFILE

Clement Osei Akoto
3 PUBLICATIONS **38** CITATIONS
SEE PROFILE

Synthesis, Structure, and Nonlinear Optical Properties of Cross-Conjugated Perphenylated *iso*-Polydiacetylenes

Yuming Zhao,[a] Aaron D. Slepkov,[b] Clement Osei Akoto,[c] Robert McDonald,[d] Frank A. Hegmann,*[b] and Rik R. Tykwinski*[c]

Abstract: Monodisperse, cross-conjugated perphenylated *iso*-polydiacetylene (*iso*-PDA) oligomers, ranging from monomer **15** to pentadecamer **25**, have been synthesized by using a palladium-catalyzed cross-coupling protocol. Structural characteristics elucidated by X-ray crystallographic analysis demonstrate a non-planar backbone conformation for the oligomers due to the steric interactions between alkylidene phenyl groups. The electronic absorption spectra of the oligomers show a slight red-shift of the maximum absorption wavelength as the chain length increases from dimer **17b** to pentadecamer **25**, a trend that has saturated by the stage of nonamer **22**. Fluorescence spectroscopy confirms that the pendent phenyl groups present on the oligomer framework enhance emission, and the relative emission intensity consistently increases as a function of chain length *n*. The molecular third-order nonlinearities, γ, for this oligomer series have been measured via differential optical Kerr effect (DOKE) detection and show a superlinear increase as a function of the oligomer chain length *n*. Molecular modeling and spectroscopic studies suggest that *iso*-PDA oligomers ($n>7$) adopt a coiled, helical conformation in solution.

Keywords: cross conjugation · enynes · foldamers · nonlinear optics · optical Kerr effect · polydiacetylenes

Introduction

Organic compounds continue to be desirable materials candidates for optical and opto-electronic applications,[1] and organic NLO materials with large molecular hyperpolarizability would be particularly useful for the fabrication of all-optical signal processing/switching devices.[2] The realization of such devices could substantially improve the capability of modern computing and telecommunications technologies. In the past several decades, enormous efforts have focused on molecules with extensive π-delocalization that often afford large nonlinear optical responses, that is, large molecular first and second hyperpolarizabilities (β and γ).[1,3] Conjugated oligomers are also attractive as nonlinear optical materials due to their extended π-electron systems.[4] For example, polyynes,[5] polyacetylenes (PAs),[6] polydiacetylenes (PDAs),[7] polytriacetylenes (PTAs),[8] as well as many others have been explored.[9] One disadvantage of linearly conjugated oligomers, however, is the dramatic red-shift of the maximum electronic absorption wavelength (λ_{max}) towards the visible region of the spectrum as the oligomer chain length is increased. This results in longer oligomers with considerably decreased transparency in the visible region of the spectrum.[10] To circumvent this "transparency-nonlinearity trade-off", alternatives to linear conjugation have been explored,[3] such as two-dimensional conjugation[11] and the substitution of functional groups in the oligomer backbones.[12]

In this context, cross-conjugated enyne oligomers[13,14] have been examined with the following motives in mind: 1) The red-shift of λ_{max} can be mediated, on account of the

[a] Prof. Y. Zhao
Department of Chemistry
Memorial University of Newfoundland
St. John's, NL A1B 3X7 (Canada)

[b] A. D. Slepkov, Prof. F. A. Hegmann
Department of Physics, University of Alberta
Edmonton, AB T6G 2J1 (Canada)
Fax: (+1) 780-492-0714
E-mail: hegmann@phys.ualberta.ca

[c] C. O. Akoto, Prof. Dr. R. R. Tykwinski
Department of Chemistry, University of Alberta
Edmonton, AB T6G 2G2 (Canada)
Fax: (+1) 780-492-8231
E-mail: rik.tykwinski@ualberta.ca

[d] Dr. R. McDonald
X-Ray Crystallography Laboratory
Department of Chemistry
University of Alberta
Edmonton, AB T6G 2G2 (Canada)

Supporting information for this article is available on the WWW under http://www.chemeurj.org/ or from the author.

 DOI: 10.1002/chem.200400822

attenuated π-electron delocalization via a cross-conjugated framework, yielding electronic transparency, even for extended oligomers, and 2) cross-conjugated oligomers remain rich in π-electron density, which is essential for providing large third-order molecular and bulk nonlinear optical susceptibilities.

Oligomers with a cross-conjugated enyne framework, such as *iso*-polydiacetylenes (*iso*-PDAs) **1** and **2**[15] and *iso*-polytriacetylenes (*iso*-PTAs),[16,17] have been studied previously.[18] These studies show that electronic communication is observed along the cross-conjugated enyne frameworks and that the oligomers also demonstrate high transparency in the visible region of the spectrum.[19] The pendant alkyl substituents (e.g., isopropylidene **1** and adamantylidene **2**), however, did not supply sufficient stability and solubility for extensive studies of nonlinear optical properties. In a quest for oligomers more suitable for study of third-order NLO behavior, a series of perphenylated *iso*-PDA oligomers **3** was targeted. It was also envisioned that both the stability and solubility (processabiltiy) could be improved.[15–17] The synthesis, spectroscopic, nonlinear optical, and conformational properties of these new oligomers are detailed in this paper.

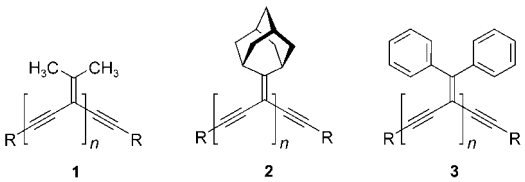

iso-polydiacetylenes

Results and Discussion

Synthesis: Friedel–Crafts acylation[20] of silyl-protected acetylenes **4–6** with diphenylacetyl chloride **7** gave ketones **8–10**, and triflation[21] under standard conditions gave the vinyl triflate building blocks **11–13** (Scheme 1). In the synthesis of ketone **8**, a mixture of bis and mono-acylated products was formed, and desilylation of ketone **8** under the reaction conditions was also observed. Replacing one of acetylenic protecting groups with a more robust triethylsilyl (TES) or triisopropylsilyl (TIPS) group, however, reduced these troublesome side-reactions during acylation and greatly facilitated the purification of ketones **9** and **10**. Since ketones **8–10** showed limited stability, even when stored under inert gas and at low temperature (−20 °C), transformation into the corresponding vinyl triflates **11–13** was immediately effected.

With the pure vinyl triflates in hand, the cross-conjugated perphenylated *iso*-PDA oligomers were prepared via an iterative cross-coupling strategy.[22,23] Whereas the synthesis of alkyl substituted enediynes **1** and **2** was accomplished under Pd-catalyzed cross-coupling conditions at room temperature,[15] the analogous reactions of triflates **12–13** with trimethylsilylacetylene **14** proceeded at an unbearably slow rate, likely due to the increased steric demands of the phenyl substituents (Scheme 2). Increasing the reaction temperature to

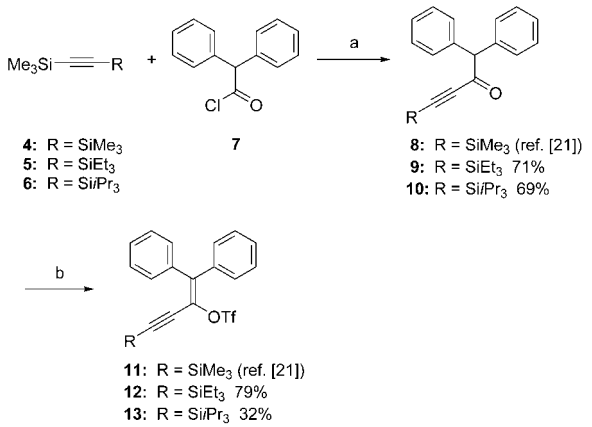

Scheme 1. Synthesis of vinyl triflate building blocks **11–13**. a) $AlCl_3$, CH_2Cl_2, 0 °C; b) triflic anhydride, 2,6-di(*tert*-butyl)-4-methylpyridine, CH_2Cl_2, RT.

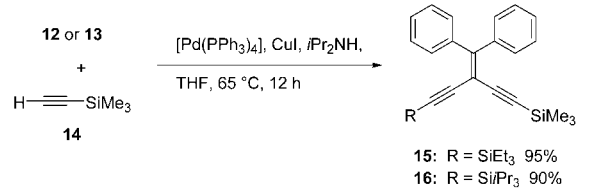

Scheme 2. Synthesis of perphenylated *iso*-PDA monomers **15** and **16**.

60–65 °C (reflux), however, led to substantially accelerated reaction rates and excellent yields of enediynes **15** and **16**, respectively.

Initial efforts to assemble perphenylated *iso*-PDA oligomers were directed toward dimer **17a** (Scheme 3). Monomer **16** was selectively desilylated and cross-coupled with triflate **13** by using $[PdCl_2(PPh_3)_2]$ as the catalyst, but this reaction consistently gave almost exclusively the homocoupled product **18a**. Attempts to optimize the dimer formation were then directed toward the formation of dimer **17b**. The TMS group of **15** was carefully removed with catalytic K_2CO_3 in MeOH/THF, and the mono-deprotected product cross-coupled with triflate **12**. Using $[PdCl_2(PPh_3)_2]$ as the catalyst, this reaction also resulted in a substantial amount of dimer **18b**. Switching to $[Pd(PPh_3)_4]$ as the catalyst, however, substantially reduced the yield of **18b** (ca. 3%) and afforded an excellent yield of **17b**. To date, the optimized cross-coupling conditions for these and subsequent reactions used $[Pd(PPh_3)_4]$ as the catalyst, CuI as the co-catalyst, iPr_2NH as the base in THF under positive Ar pressure, at reflux for at least 12 h.

Exhaustive deprotection of **15** with tetrabutylammonium fluoride (TBAF) gave the bisterminal alkyne, which was cross-coupled with triflate **12** to afford trimer **19** as a yellow solid (Scheme 4). Repetition of the protiodeprotection and cross-coupling sequence then afforded pentamer **20** and heptamer **21** in respectable yields. Further elaboration of heptamer **21** afforded nonamer **22**, and while **22** shows decent solubility in organic solvents, purification via column chromatography (silica gel or alumina) was problematic be-

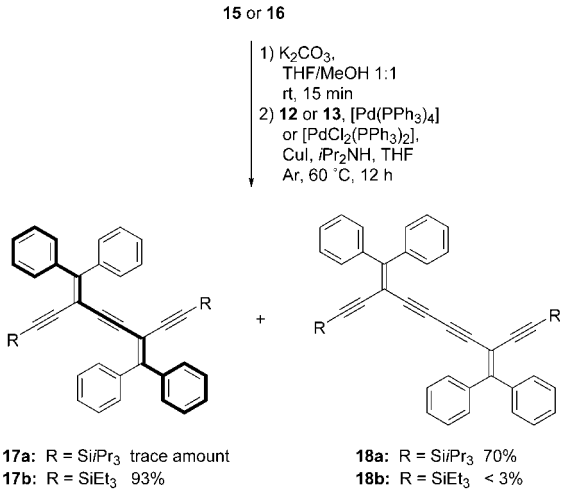

Scheme 3. Synthesis of dimeric perphenylated *iso*-PDAs.

cause of significant aggregation of the various products. Size-exclusion chromatography (SEC) thus proved to be invaluable in the purification of nonamer **22**, as well as longer oligomers, by using CH_2Cl_2 as an eluent. This general protocol led to good yields of undecamer **23**, tridecamer **24** and pentadecamer **25**. Compound **25** is the longest monodisperse *iso*-PDA oligomer synthesized to date, and it consists of a cross-conjugated enyne backbone composed of 62 sp and sp^2 hybridized carbons.

It was only in the transformation of **15** to **19** where an isolable amount of a homocoupled by-product **26** was also isolated (8%). Although small amounts of such by-product(s) were also detected in subsequent reactions, the compounds were extremely difficult to isolate pure because of the small quantity of material.

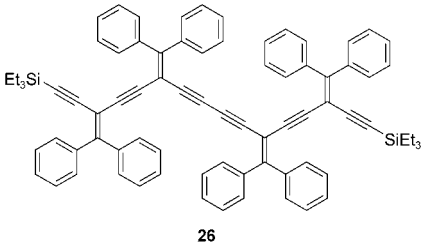

26

Characterization: Electrospray mass spectrometry (ESIMS) proved to be a particularly powerful tool for characterization of the oligomers. For all compounds, a clear signal for $[M+X]^+$ (X = Na and/or Ag) was observed in analysis (positive mode) of MeOH/toluene solutions with added AgOTf. For example, analysis of the tridecamer **24** shows a signal at *m*/*z* 2991 as expected for $[M+Ag]^+$, and that of pentadecamer **25** shows *m*/*z* 3309 and 3392, consistent with $[M+Na]^+$ and $[M+Ag]^+$, respectively.

In the ^{13}C NMR spectra of the *iso*-PDA oligomers, the resonances of the alkylidene carbons outside of the main chain (Ph_2C=C) are the most easily identified, resonating quite downfield in a range of 155–158 ppm. In the spectrum of heptamer **21**, these four carbons remain discernible at δ 154.9, 155.1, 155.4, and 156.9. For the longer oligomers, however, chemical shift degeneracy of these carbons exists, that is, only five of seven are distinguishable for tridecamer **24**, and only four of eight can be seen for **25**. The in-chain alkylidene carbons (Ph_2C=C) fall farther upfield, in the chemical shift range of the acetylenic carbons. For the longer oligomers, significant chemical shift degeneracy is also observed for resonances of sp and sp^2 carbons of the enyne framework (even when measured at 125 MHz). For instance, already in the spectrum of pentamer **20**, only 11 of 12 unique sp and sp^2 carbon resonances (excluding the phenyl carbons) are discernible.

All *iso*-PDA oligomers show reasonable thermal stability. Dimer **17b**, trimer **19**, pentamer **20**, and heptamer **21** show well defined melting points at 67–69, 60–61, 85–86, and 124–126 °C, respectively. Nonamer **22**, undecamer **23**, tridecamer **24**, and pentadecamer **25** decompose at 134–135, 140–142, 148–150, and 155–159 °C, re-

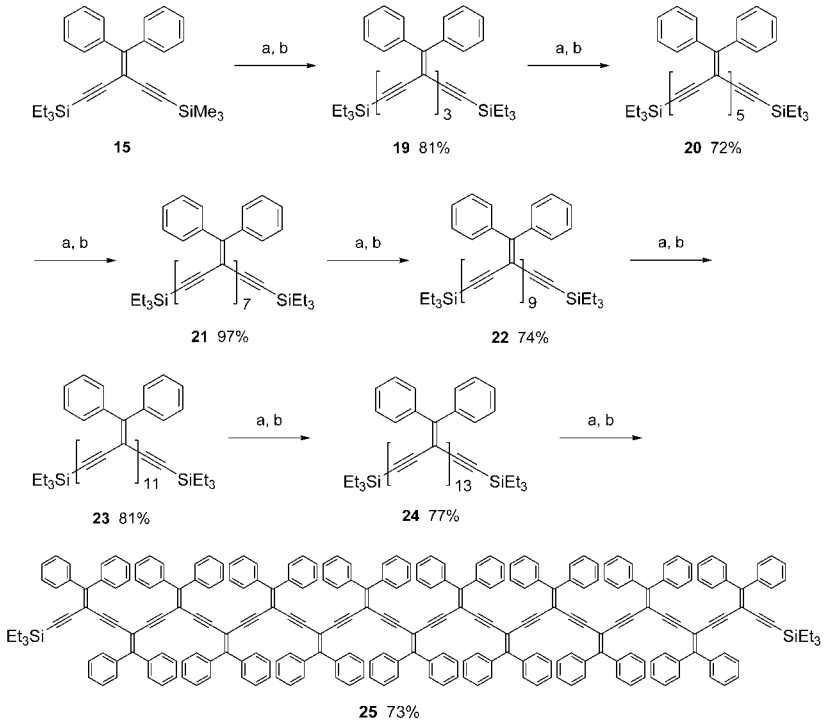

Scheme 4. Iterative synthesis of perphenylated *iso*-PDAs **19**–**25**. a) TBAF, wet THF, RT; b) **12**, $[Pd(PPh_3)_4]$, CuI, iPr_2NH, THF, reflux, 12 h.

spectively. Differential scanning calorimetric (DSC) analysis of these longer oligomers confirmed the decomposition. In comparison to the alkyl substituted *iso*-PDAs (i.e., oligomers **1** and **2**),[15] the perphenylated oligomers exhibited substantially improved kinetic stability and no significant decomposition could be detected by either TLC or NMR spectroscopic analysis for samples exposed to ambient conditions for several weeks.

Solid-state structural properties: Crystallographic analyses of monomer **15**, dimer **17b**, trimer **19**, and homocoupled dimer **18a** were performed to examine the solid-state structural characteristics of the *iso*-PDA oligomers. While disorder, particularly in the ethyl groups, hampered the refinement of the data for **15** (Figure 1), the resulting structure is sufficient for an empirical analysis and as a point of comparison to that of the other oligomers. The alkylidene angle C2-C3-C5 at 114.3(3)° is comparable to the that of its isopropylidene analogue at 112.9(4)°.[15] Both SiC≡C bond angles, at 172.2(3) and 174.9(4)°, are distorted from linearity, presumably due to crystal packing effects. Steric interactions between the two alkylidene phenyl groups prohibit co-planarity and force the phenyl rings out of the enediyne plane by 47.7(6) and 43.0(6)°.

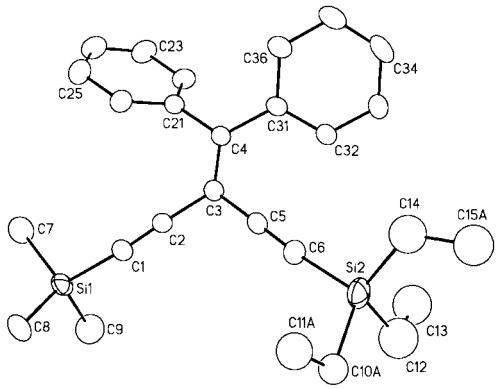

Figure 1. ORTEP drawing (20% probability level) of **15**. Selected bond angles [°]: Si1-C1-C2 172.2(3), C1-C2-C3 176.9(4), C2-C3-C5 114.3(3), C3-C5-C6 177.5(4), C21-C4-C31 116.8(3), Si2-C6-C5 174.9(4).

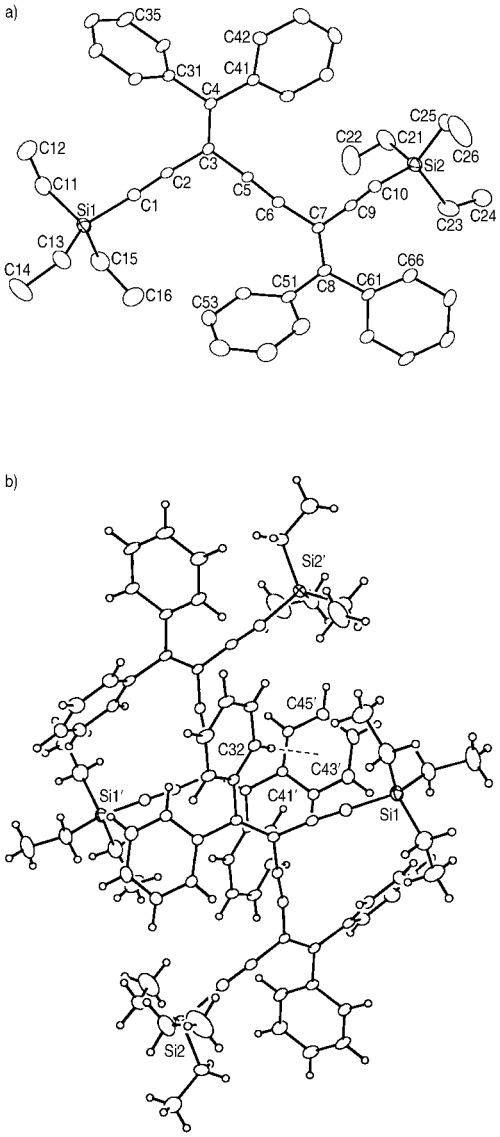

Figure 2. a) ORTEP drawing (20% probability level) of **17b**. Selected bond angles [°]: Si1-C1-C2 175.4(3), C1-C2-C3 175.4(4), C2-C3-C5 113.9(3), C3-C5-C6 176.5(4), C5-C6-C7 171.6(3), C6-C7-C9 113.6(3), C7-C9-C10 176.8(4), Si2-C10-C9 172.7(3); b) crystal packing of **17b**.

Crystallographic analysis of dimer **17b** shows a pseudo s-*trans* orientation of the two olefins about the central acetylenic bond and a nonplanar the enyne framework (Figure 2). The dihedral angle between the two alkylidene least-squares planes, namely plane 1 (C2, C3, C4, and C5) and plane 2 (C6, C7, C8, and C9), is 33.70(16)°. The two enediyne alkylidene angles at 113.9(3) and 113.6(3)° are similar to that of monomer **15**. The packing diagram of **17b** shows that the distance between H(32) and phenyl plane (C41′, C42′, C43, C44′, C45′, C46′) is 3.26 Å, which is an indication of the intermolecular π-stacking in a "face-to-edge" manner or "T-stacking" (Figure 2b).[24,25]

Crystallographic analysis of trimer **19** shows that the cross-conjugated oligoenyne framework does not assume a planar conformation due to the steric interactions between the phenyl groups of neighboring alkylidene moieties. Notably, trimer **19** shows a pseudo-*cis*-*trans* orientation rather than an all s-*trans* orientation; the only *iso*-PDA to date that displays a cisoid orientation for neighboring alkylidene groups in the solid state (Figure 3). The intramolecular distance between H(55) and H(56) to phenyl plane 4 (C61, C62, C63, C64, C65, C66) is observed at 3.20 and 3.37 Å, respectively, with an angle between the two phenyl planes is 79°. This orientation suggests π-stacking of the "face-to-edge" type that stabilizes the pseudo-*cis* orientation in the solid state.

The cross-conjugated enyne framework of **18a** (Figure 4) shows a transoid, centrosymmetric, and nearly planar conformation (C_{2h} symmetry), with a maximum deviation of 0.078(2) Å from the least-squares plane (excluding the

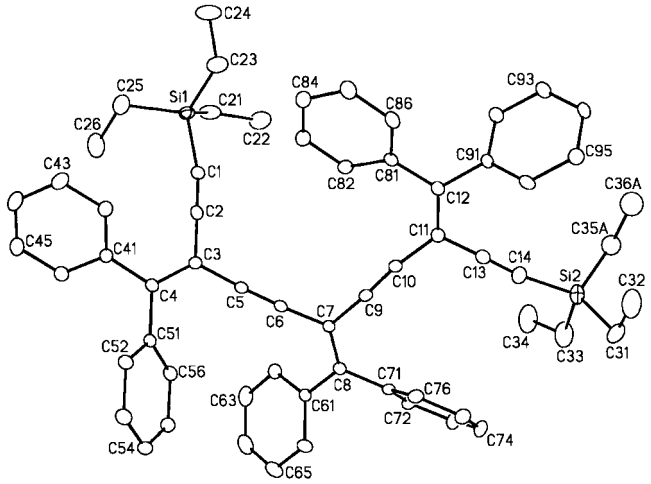

Figure 3. ORTEP drawing (20% probability level) of **19**. Selected bond angles [°]: Si1-C1-C2 168.9(3), C1-C2-C3 176.5(3), C2-C3-C5 114.4(3), C3-C5-C6 176.8(3), C5-C6-C7 175.1(3), C6-C7-C9 114.2(3), C7-C9-C10 174.4(4), C9-C10-C11 170.4(3), C10-C11-C13 113.0(3), C11-C13-C14 177.5(4), Si2-C14-C13 172.2(3).

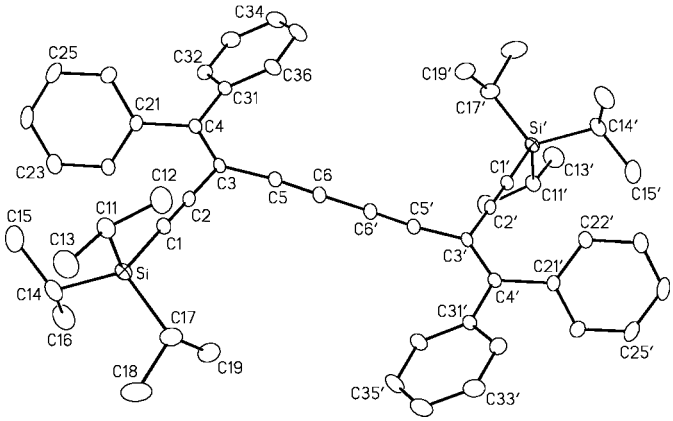

Figure 4. ORTEP drawing (20% probability level) of **18a**. Selected bond angles [°]: Si1-C1-C2 178.2(2), C1-C2-C3 176.2(3), C2-C3-C5 115.13(19), C3-C5-C6 174.4(3), C5-C6-C6′ 178.7(3).

phenyl and silyl moieties). It is clear that the central butadiynyl linkage sufficiently distances the alkylidene moieties such that steric interactions are relieved, resulting in a fully planar enyne conformation in the solid state.

Compound **18a** shows a parallel stacking arrangement in the solid state (Figure 5), with solid-state packing parameters for the central butadiynyl moieties of $\Phi = 35°$, $R_{1,4} = 6.1$ Å, $d = 8.6$ Å. When compared to the optimal parameters for topochemical polymerization of butadiynes in a 1,4-addition fashion, $\Phi = 45°$, $R_{1,4} < 4.0$ Å, $d = 5.0$ Å, however,[26] there is little possibility for reaction, since the distance between neighboring molecules is too great. In the packing of **18a**, it is interesting to note that there are no intermolecular and/or intramolecular π-stacking interactions observed between proximal phenyl groups.

Electronic absorption and emission: The electronic absorption characteristics of dimer **17b** through pentadecamer **25** were investigated by UV/Vis spectroscopy (Figure 6). The most obvious aspect of the UV/Vis spectra is the steadily increasing molar absorptivity as the chain length is extended, which ultimately reaches $\varepsilon = 160000$ for *iso*-PDA **25**. The spectrum of dimer **17b** shows two distinct absorptions at 373 and 323 nm. In the absence of a significant contribution from cross-conjugation, the major absorptions for **17b**, as well as the other *iso*-PDAs, are expected to arise from the longest linearly conjugated framework, ene-yne-ene segment shown in bold in Scheme 3.[27] Previous work with cyclic *iso*-PDAs suggests that the lower energy absorption (373 nm) results from the HOMO→LUMO transition for both the cisoid and transoid conformers of this ene-yne-ene segment, with the cisoid absorption occurring at slightly higher energy than the transoid. It is predicted that absorption at 323 nm arises from the HOMO→LUMO + 1 transition of the cisoid conformer, a transition that is formally symmetry forbidden for the transoid conformer.[15] The spectrum of trimer **19** shows a similar absorption profile to that of **17b**, with distinctive absorptions at 375 and 324 nm. In the spectrum of pentamer **20**, the low-energy absorption at 377 nm becomes the only notable characteristic, as the higher-energy absorption at 324 nm merges into a barely distinguishable shoulder. From heptamer **21** to pentadecamer **25**, the absorption profiles show a broad and featureless absorption at $\lambda_{max} = 378$ nm. Overall, a slight lowering of the λ_{max} value versus chain length is observed dimer **17b** ($\lambda_{max} = 373$ nm) to pentadecamer **25** ($\lambda_{max} = 378$ nm). This effect has, however, already reached saturation by the length of about $n = 7$–9, similar to that of *iso*-PDAs **1**.[15]

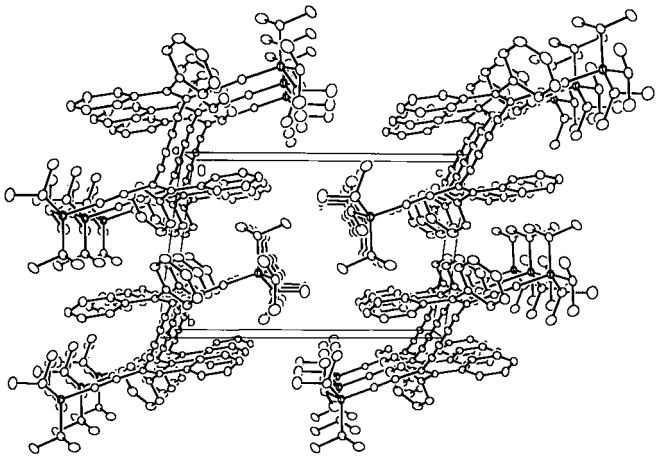

Figure 5. Crystal packing diagram of **18a** viewed along *b* axis.

The influence of solvent polarity on the electronic absorptions was investigated using nonamer **22**. In most cases, only a slight change of λ_{max} (ca. 3 nm) was found. For example, in $CHCl_3$, hexanes, and benzene $\lambda_{max} = 377$ nm, whereas in Et_2O and THF $\lambda_{max} = 374$ nm. The absorption profiles are also similar to each other. The UV/Vis spectrum of **22** in acetonitrile, however, shows obvious differences when compared with those from other solvents. In acetonitrile, the lowest energy absorption has shifted toward higher energy

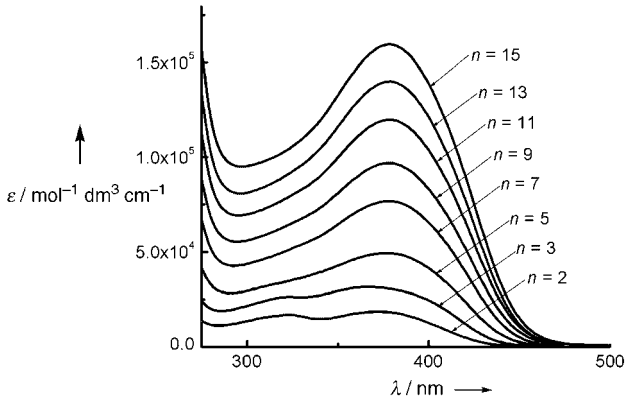

Figure 6. Electronic absorption spectra in $CHCl_3$ comparing the effects of oligomer chain length between **17b**, **19**–**25**.

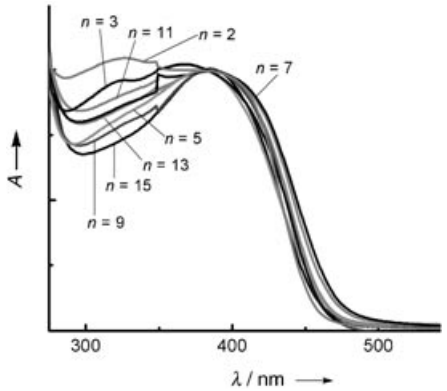

Figure 7. Solid state UV/Vis spectra for **17b** and **19**–**25** as thin films cast from $CHCl_3$ onto quartz slides.

by about 12 nm ($\lambda_{max}=365$ nm), and the high energy absorption at 323 nm, as observed in the spectra of dimer **17b** and trimer **19** in $CHCl_3$, is also discernible.[28] This observed behavior in CH_3CN is analogous to that observed for the folding of oligo(*m*-phenylene ethynylene) systems reported by Moore and co-workers[29] and will be discussed in more detail below.

UV/Vis spectra of *iso*-PDA oligomers **21** and **22** were recorded at varied concentrations (from 10^{-5} to 10^{-7} M) in $CHCl_3$ in order to probe the possibility of aggregation in solution. These results showed consistent profiles and nearly identical extinction coefficients, suggesting little or no aggregation over the accessible range of concentrations.

The absorption spectra of *iso*-PDA oligomers as thin films cast from $CHCl_3$ onto quartz slides were measured (Figure 7). The oligomers form reasonably good quality thin films with absorption profiles that are similar to those measured in solution. Thus, no pronounced *intermolecular* aggregation band could be detected.[30] The slight random change in λ_{max} values observed in the spectra of the films was presumably due to scattering effects and slight variances in the films.

Emission spectra were measured in degassed $CHCl_3$ with an excitation wavelength of 380 nm (Figure 8), and the perphenylated *iso*-PDAs show enhanced emission when compared to their alkylidene analogues **1** and **2**.[31] All oligomers show only one broad emission peak, and the relative intensity steadily increases with chain length. The maximum emission wavelength (λ_{em}) shifts toward lower-energy in the progression from dimer **17b** ($\lambda_{em}=468$ nm) to heptamer **21** ($\lambda_{em}=503$ nm). From heptamer **21** to pentadecamer **25**, λ_{em} maintains an essentially constant value. This trend concurs with that observed for the UV/Vis absorption data, suggesting an effective conjugation length (ECL) of $n_{ECL}\approx 7$.

Nonlinear optical properties: One of the most appealing aspects of these new *iso*-PDA oligomers is their potential as third-order NLO materials because of their significant optical transparency. The molecular second hyperpolarizabilities, γ_s, for the *iso*-PDA samples were determined by differential

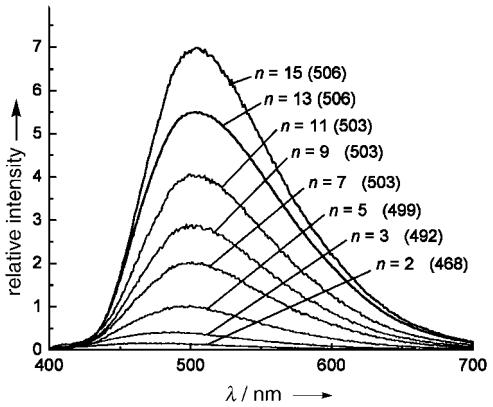

Figure 8. Emission spectra in $CHCl_3$ for **17b** and **19**–**25** (excitation at 380 nm); λ_{em} [nm] for each oligomer is shown in parentheses.

optical Kerr effect (DOKE) experiments.[14a,b] In these experiments, the oligomer samples, from monomer **15** to pentadecamer **25**, were prepared as THF solutions of 0.035–0.23 M. The γ_s values were then obtained as previously described,[14a,b] and all the γ_s values are referenced to that of THF (γ_{THF}). A summary of the γ_s values for the entire oligomer series are listed in Table 1.

As depicted by the values in Table 1, the *iso*-PDA series shows an order of magnitude increase in γ_s from the dimer **17b** to pentadecamer **25**, although the γ_s values themselves

Table 1. DOKE results for the *iso*-PDA series.[a]

Entry	*n*	*c* [M]	γ_s ($\times 10^{-36}$ esu)	γ_s/γ_{THF}
15	1	0.23	9.2 ± 0.4	17.7 ± 0.8
17b	2	0.15	30.3 ± 0.3	58.2 ± 0.5
19	3	0.13	48 ± 4	94 ± 7
20	5	0.12	70 ± 5	134 ± 9
21	7	0.10	94 ± 4	181 ± 9
22	9	0.12	123 ± 8	240 ± 15
23	11	0.054	177 ± 18	347 ± 35
24	13	0.054	208 ± 10	408 ± 20
25	15	0.035	308 ± 8	603 ± 16

[a] γ_s and γ_{THF} are the second hyperpolarizabilities of the oligomer samples and THF reference, respectively; *n* is the number of repeat units in the oligomer.

remain quite modest. On the basis of the absorption and emission data, conventional wisdom dictates that limited electronic communication is found across a cross-conjugated bridge. Thus, increasing the number of repeat units would simply increase the number of fixed-length linearly-conjugated paths (as shown in bold, Scheme 3). In the absence of significant cross-conjugated π-delocalization, this would afford a linear increase in γ_s values as a function of chain length. Indeed, a linear trend for shorter *iso*-PDA oligomers ($n=2$–7) was observed.[14a,b] Extending this investigation to longer oligomers, however, revealed markedly different behavior as shown in Figure 9a, where the oligomer nonlinearities clearly increase superlinearly with respect to chain length.

A superlinear increase in γ values as a function of chain length is encountered in both theoretical and experimental studies of linearly conjugated oligomers. These studies have shown that optical nonlinearities typically increase with conjugated length according to a power-law relationship, $\gamma \sim n^c$, where c is the power law exponent.[32,33] Furthermore, a fit of the data to expressions of the form $\gamma \sim n^c$ is an indication of increased electronic communication along a conjugated backbone. While theories predict power law exponents of $c=2$–4 for linearly conjugated systems, there are currently no theoretical predictions for cross-conjugated systems. Figure 9b presents the data of *iso*-PDA series fit to a power law function of the form $\gamma = a + bn^c$, where a and b are constants. This analysis provides a superior fit to a simple straight line, yielding a power of $c=2.0\pm0.3$. While the data adequately fits a power-law, the correlation is not, however, ideal.

A third possible relationship, consisting of two linearly increasing regimes is considered as shown in Figure 9c. The γ_s values show a good linear fit spanning $n=2$–7 and a second linear fit with a steeper slope over the range of $n=9$–15. Overall, the two-line analysis with a distinct change in slope at $n\approx9$, provides the best description of the data.

The analyses in Figures 9b and c would be explained by two different phenomena. A power-law relationship between γ and oligomer length (Figure 9b) would presumably arise from increased π-electron delocalization, a surprising prospect considering the UV/Vis absorption and emission data found for the *iso*-PDAs. A superlinear increase in nonlinearities with a distinct change in slope, however, could arise from an increased ordering of the sample in solution, such as folding.[34] This prospect is discussed below.

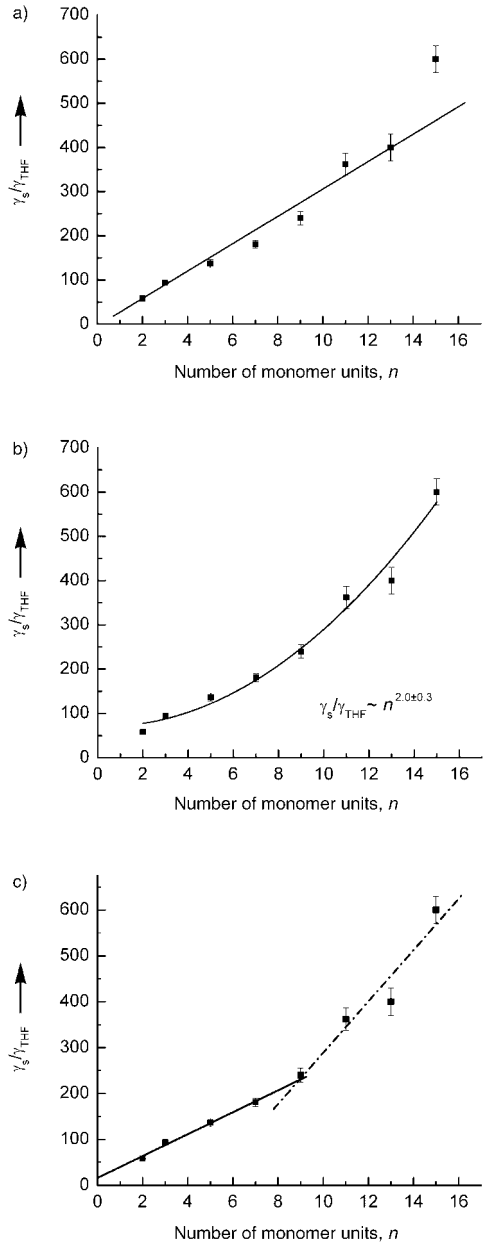

Figure 9. Correlation of relative molecular second hyperpolarizabilities (γ_s/γ_{THF}) as a function of oligomer length n. a) Linear fit ($n=2$–15). b) Power-law fit of the form $\gamma=a+bn^c$ ($n=2$–15). c) Two linear fits ($n=$ 2–7 and 9–15).

Solution state folding of *iso*-PDAs: The interesting results from the NLO analyses suggested that the perphenylated *iso*-PDA oligomers might prefer a specific, folded, conformation in the solution state when $n>7$. This suggestion is also supported by the crystallographic analysis of trimer **19**, where the pseudo-*cis* orientation between enediyne segments allows the neighboring phenyl groups to approach close enough to effect π–π interactions, which could become a dominant feature in the longer oligomers.

The geometry of *iso*-PDA oligomers of various length was analyzed computationally.[35] When the initial oligomer geometry adopts an all-*cisoid* conformation ($n>7$), the minimized structure consistently converged to a helical conformation with a "folded" enyne framework (Figure 10a). The phenyl rings of neighboring alkylidene units each participate in π-stacking, which contributes to stabilization of the folded conformation (Figure 10b). The pitch angle for the helix is calculated to be approximately 40°.

Folding of the oligomers is also supported by UV/Vis spectroscopic analysis. Previous work on *iso*-PDAs provide for the following assumptions: a) The HOMO→LUMO+1 transition at about 323 nm is symmetry allowed for the cisoid conformation and forbidden for the transoid confor-

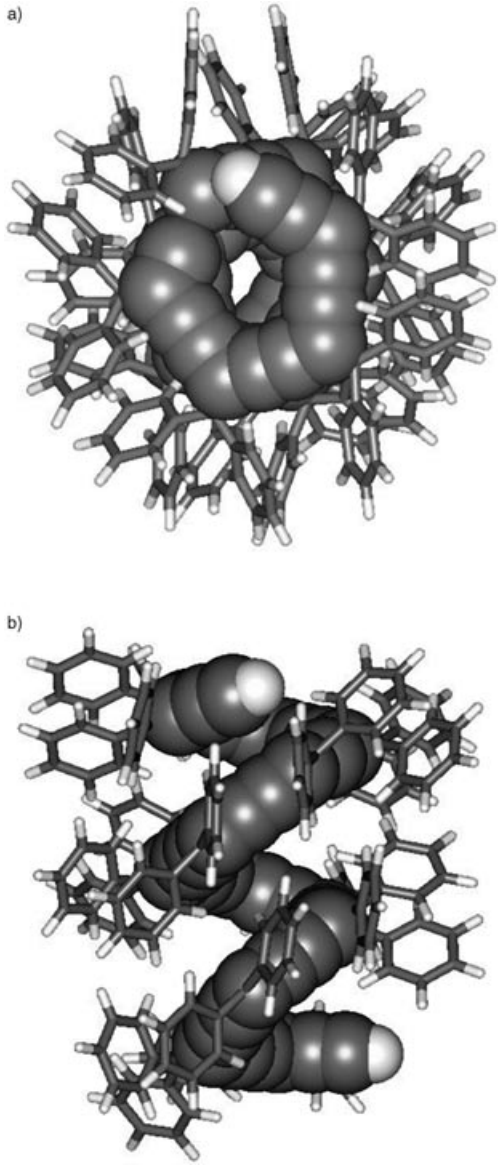

Figure 10. Minimized structure of tridecameric *iso*-PDA using MM3* force field parameters. Only backbone carbons are displayed as space-filling representation for clarity: a) View from top; b) view from side.

mation,[15] and b) the HOMO→LUMO transition for the cisoid ene-yne-ene chromophore occurs at slightly higher energy than that of the transoid conformer (although both are observed as a combined absorption band at about 378 nm in the present case).[15,36] The ratio of these two absorbances (denoted as A_{378}/A_{323}) could therefore be an indicator of conformation change, and a plot of this indicator versus chain length n is presented in Figure 11. In both $CHCl_3$ and acetonitrile, the ratio of A_{378}/A_{323} steadily increased from dimer **17b** to heptamer **21**, and then reached a constant value for the longer oligomers ($n \geq 7$). In an effort to provide additional support of a folded conformation, circular dichroism (CD) spectroscopy was also explored, as established by Moore and co-workers,[37] including the use of chiral solvents as well as attempts to incorporate a chiral

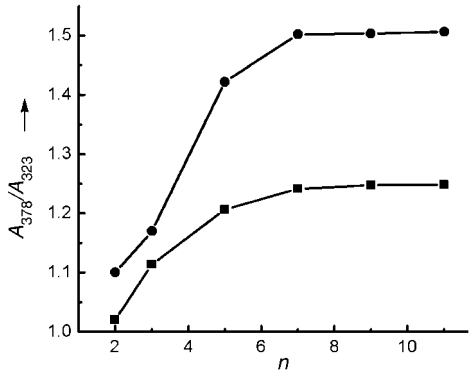

Figure 11. Plot of absorbance ratio A_{378}/A_{323} vs chain length (n) in $CHCl_3$ (●) and acetonitrile (■). A_{378} denotes the absorbance intensity at 378 nm, and A_{323} denotes the absorbance intensity at 323 nm.

guest molecule. These studies, unfortunately, did not give conclusive evidence for (or against) solution-state folding, as a biased twist sense could not be achieved.

Conclusion

An efficient synthesis for perphenylated cross-conjugated *iso*-PDAs ($n = 1$–15) has been developed by using an iterative divergent route. The oligomers were synthesized and purified in satisfactory yields as stable and soluble solids. Solid-state properties of monomer **15** to trimer **19**[38] were analyzed by X-ray crystallography and show that these oligomers prefer non-planar conformations due to the steric demands from the phenyl groups. Their electronic absorption behavior indicates an effective conjugation length of $n_{ECL} = 7$–9. *iso*-PDA oligomers show steadily increasing fluorescence intensity as a function of chain length, and the emission wavelength shifts slightly from 468 nm (dimer **17b**) to 503 nm (heptamer **21**). Beyond the length of the heptamer, the emission energy remains essentially constant. The third-order NLO properties of the *iso*-PDAs in THF solutions were studied by differential optical Kerr effect (DOKE) experiments. Molecular second hyperpolarizabilities, γ_S, give a super-linear increase as a function of chain length. The best fit to the NLO data shows two linear regimes, suggesting an increased order in the system, likely folding. While definitive proof of a folded conformation for extended *iso*-PDAs remains elusive, empirical evidence of this conformational presence is provided by molecular modeling studies as well as UV/Vis spectroscopy. Additional studies of conformation, as well as the synthesis of chiral and optically pure *iso*-PDA derivatives, are currently underway.

Acknowledgement

This research was supported by the University of Alberta, the Natural Sciences and Engineering Research Council of Canada, Canada Foundation for Innovation, IIPP, ASRA, CIPI, iCORE, and Petro-Canada

(Young Innovator Award to RRT). Drs. R. M. Whittal and A. Morales-Izquierdo are gratefully acknowledged for mass spectrometric characterization, and Drs. R. Lam and M. Wang for assisting with determining the crystal structures of compound **15** and **17b**, respectively.

[1] a) C. Bosshard, K. Sutter, P. Prêtre, J. Hulliger, M. Flörsheimer, P. Kaatz, P. Günter, *Organic Nonlinear Optical Materials*, *Vol. 1*, Gordon and Breach, Amsterdam, **1995**; b) *Nonlinear Optics of Organic Molecules and Polymers* (Eds.: H. S. Nalwa, S. Miyata), CRC Press, Boca Raton, **1997**; c) P. N. Prasad, D. J. Williams, *Introduction to Nonlinear Optical Effects in Molecules and Polymers*, Wiley, New York, **1991**.

[2] a) B. Luther-Davies, M. Samoc, *Curr. Opin. Solid State Mater. Sci.* **1997**, *2*, 213–219; b) *Principles and Applications of Nonlinear Optical Materials* (Eds.: R. W. Munn, C. N. Ironside), CRC Press, Boca Raton, **1993**.

[3] a) U. Gubler, C. Bosshard, *Adv. Polym. Sci.* **2002**, *158*, 123–191; b) R. R. Tykwinski, U. Gubler, R. E. Martin, F. Diederich, C. Bosshard, P. Günter, *J. Phys. Chem. B* **1998**, *102*, 4451–4465.

[4] a) *Electronic Materials: The Oligomer Approach* (Eds.: K. Müllen, G. Wegner), VCH, Weinheim, **1997**; b) R. E. Martin, F. Diederich, *Angew. Chem.* **1999**, *111*, 1440–1469; *Angew. Chem. Int. Ed.* **1999**, *38*, 1350–1377.

[5] A. D. Slepkov, F. A. Hegmann, S. Eisler, E. Elliott, R. R. Tykwinski, *J. Chem. Phys.* **2004**, *120*, 6807–6810.

[6] a) S. Hahn, D. Kim, M. Cho, *J. Phys. Chem. B* **1999**, *103*, 8221–8229; b) A. Kiehl, A. Eberhardt, M. Adam, V. Enkelmann, K. Müllen, *Angew. Chem.* **1992**, *104*, 1623–1626; *Angew. Chem. Int. Ed. Engl.* **1992**, *31*, 1588–1591.

[7] M. P. Carreon, L. Fomina, S. Fomine, D. Rao, F. J. Aranda, T. Ogawa in *Photonic and Optoelectronic Polymers, ACS Symp. Series*, *Vol. 672* (Eds.: S. A. Jenekhe, K. J. Wynn), **1997**, pp. 199–216.

[8] R. E. Martin, U. Gubler, J. Cornil, M. Balakina, C. Boudon, C. Bosshard, J.-P. Gisselbrecht, F. Diederich, P. Günter, M. Gross, J.-L. Brédas, *Chem. Eur. J.* **2000**, *6*, 3622–3635.

[9] See for example, a) L. Kuang, Q. Y. Chen, E. H. Sargent, Z. Y. Wang, *J. Am. Chem. Soc.* **2003**, *125*, 13648–13649; b) M. S. Wong, Z. H. Li, M. F. Shek, M. Samoc, A. Samoc, B. Luther-Davies, *Chem. Mater.* **2002**, *14*, 2999–3004; c) K. Ogawa, T. Zhang, K. Yoshihara, Y. Kobuke, *J. Am. Chem. Soc.* **2002**, *124*, 22–23; d) P. Siemsen, U. Gubler, C. Bosshard, P. Günter, F. Diederich, *Chem. Eur. J.* **2001**, *7*, 1333–1341; e) H. Meier, D. Ickenroth, U. Stalmach, K. Koynov, A. Bahtiar, C. Bubeck, *Eur. J. Org. Chem.* **2001**, 4431–4443.

[10] a) M. Blanchard-Desce, J. B. Baudin, L. Jullien, R. Lorne, O. Ruel, S. Brasselet, J. Zyss, *Opt. Mater.* **1999**, *12*, 333–338; b) C. R. Moylan, R. J. Twieg, V. Y. Lee, S. A. Swanson, K. M. Betterton, R. D. Miller, *J. Am. Chem. Soc.* **1993**, *115*, 12599–12600; c) I. Ledoux, J. Zyss, A. Jutand, C. Amatore, *Chem. Phys.* **1991**, *150*, 117–123.

[11] a) U. Gubler, R. Spreiter, C. Bosshard, P. Günter, R. R. Tykwinski, F. Diederich, *Appl. Phys. Lett.* **1998**, *73*, 2396–2398; b) C. Bosshard, R. Spreiter, P. Günter, R. R. Tykwinski, M. Schreiber, F. Diederich, *Adv. Mater.* **1996**, *8*, 231–234.

[12] a) S. Concilio, I. Biaggio, P. Günter, S. P. Piotto, M. J. Edelmann, J. M. Raimundo, F. Diederich, *J. Opt. Soc. Am. B* **2003**, *20*, 1656–1660; b) U. Gubler, S. Concilio, C. Bosshard, I. Biaggio, P. Günter, R. E. Martin, M. J. Edelmann, J. A. Wytko, F. Diederich, *Appl. Phys. Lett.* **2002**, *81*, 2322–2324.

[13] R. R. Tykwinski, Y. Zhao, *Synlett* **2002**, 1939–1953.

[14] a) A. D. Slepkov, F. A. Hegmann, Y. Zhao, R. R. Tykwinski, K. Kamada, *J. Chem. Phys.* **2002**, *116*, 3834–3840; b) A. D. Slepkov, F. A. Hegmann, K. Kamada, Y. Zhao, R. R. Tykwinski, *J. Opt. A Pure Appl. Opt.* **2002**, *4*, S207–S211.

[15] a) Y. Zhao, R. R. Tykwinski, *J. Am. Chem. Soc.* **1999**, *121*, 458–459; b) Y. Zhao, K. Campbell, R. R. Tykwinski, *J. Org. Chem.* **2002**, *67*, 336–344.

[16] a) Y. Zhao, R. McDonald, R. R. Tykwinski, *J. Org. Chem.* **2002**, *67*, 2805–2816; b) Y. Zhao, R. McDonald, R. R. Tykwinski, *Chem. Commun.* **2000**, 77–78.

[17] E. Burri, F. Diederich, M. B. Nielsen, *Helv. Chim. Acta* **2002**, *85*, 2169–2182.

[18] For recent reports of other cross-conjugated oligomers, see: a) M. Klokkenburg, M. Lutz, A. L. Spek, J. H. van der Maas, C. A. van Walree, *Chem. Eur. J.* **2003**, *9*, 3544–3554; b) S. Fielder, D. D. Rowan, M. S. Sherburn, *Angew. Chem.* **2000**, *112*, 4501–4503; *Angew. Chem. Int. Ed.* **2000**, *39*, 4331–4333; c) M. R. Bryce, M. A. Coffin, P. J. Skabara, A. J. Moore, A. S. Batsanov, J. A. K. Howard, *Chem. Eur. J.* **2000**, *6*, 1955–1962.

[19] M. Bruschi, M. G. Giuffreda, H. P. Lüthi, *Chem. Eur. J.* **2002**, *8*, 4216–4227.

[20] a) R. M. Walton, H. Waugh, *J. Organomet. Chem.* **1972**, *37*, 45–56; b) L. Birkofer, A. Ritter, H. Uhlenbrauck, *Chem. Ber.* **1963**, *96*, 3280–3288.

[21] P. J. Stang, T. E. Fisk, *Synthesis* **1979**, 438–440.

[22] *Metal-Catalyzed Cross-Coupling Reactions* (Eds.: F. Diederich, P. Stang), VCH, Weinheim, **1998**.

[23] a) J. M. Tour, *Acc. Chem. Res.* **2000**, *33*, 791–804; b) U. H. F. Bunz, *Chem. Rev.* **2000**, *100*, 1605–1644.

[24] a) C. A. Hunter, K. R. Lawson, J. Perkins, C. J. Urch, *J. Chem. Soc. Perkin Trans. 2* **2001**, 651–669; b) C. A. Hunter, J. K. M. Sanders, *J. Am. Chem. Soc.* **1990**, *112*, 5525–5534.

[25] a) F. J. Carver, C. A. Hunter, P. S. Jones, D. J. Livingston, J. F. McCabe, E. M. Seward, P. Tiger, S. E. Spey, *Chem. Eur. J.* **2001**, *7*, 4854–4862; b) R. D. Shannon, *Acta Crystallogr.* **1976**, *A32*, 751–767.

[26] a) J.-F. Nierengarten, M. Schreiber, F. Diederich, V. Gramlich, *New J. Chem.* **1996**, *20*, 1273–1284; b) V. Enkelmann, *Adv. Polym. Sci.* **1984**, *63*, 91–136; c) G. Wegner, *Z. Naturforsch. B* **1969**, *24*, 824–832.

[27] It is worth noting, however, that a fully planar conformation is not easily achieved in longer oligomers, as demonstrated by crystallographic analyses. Accordingly, it is possible that π-electron delocalization could be, on average, mediated to a more limited segment than that shown in bold.

[28] See Supporting Information.

[29] For an excellent review of foldamers, see: D. J. Hill, M. J. Mio, R. B. Prince, T. S. Hughes, J. S. Moore, *Chem. Rev.* **2001**, *101*, 3893–4011.

[30] a) N. G. Pschirer, U. H. F. Bunz, *Macromolecules* **2000**, *33*, 3961–3963; b) C. E. Halkyard, M. E. Rampey, L. Kloppenburg, S. L. Studer-Martinez, U. H. F. Bunz, *Macromolecules* **1998**, *31*, 8655–8659.

[31] The relative maximum emission intensity (I_{max}) is only proportional to concentration in solutions less than 1.5 μM.

[32] a) U. Gubler, C. Bosshard, P. Günter, M. Y. Balakina, J. Cornil, J.-L. Brédas, R. E. Martin, F. Diederich, *Optics Lett.* **1999**, *24*, 1599–1601; b) G. P. Zhang, *Phys. Rev. B* **1999**, *60*, 11482–11486.

[33] C. Bubeck in *Electronic Materials—The Oligomer Approach* (Eds.: K. Müllen, G. Wegner), Wiley-VCH, Weinheim, **1998**, Chapter 8.

[34] Q. Huo, K. C. Russell, R. M. Leblanc, *Langmuir* **1999**, *15*, 3972–3980.

[35] Molecular mechanics software *Macromodel 7.0*, using the implemented MM3* force field parameters; the silyl groups were excluded to minimize computational time.

[36] S. Eisler, R. R. Tykwinski, *Angew. Chem.* **1999**, *111*, 2138–2341; *Angew. Chem. Int. Ed.* **1999**, *38*, 1940–1943.

[37] See, for example: a) J. C. Nelson, J. G. Saven, J. S. Moore, *Science* **1997**, *277*, 1793–1796; b) R. B. Prince, S. A. Barnes, J. S. Moore, *J. Am. Chem. Soc.* **2000**, *122*, 2758–2762.

[38] CCDC-246686 (**15**), -246687 (**17b**), -246689 (**18a**) and -246688 (**19**) contain the supplementary crystallographic data for this paper. These data can be obtained free of charge via www.ccdc.cam.ac.uk/conts/retrieving.html (or from the Cambridge Crystallographic Data Centre, 12, Union Road, Cambridge CB21EZ, UK; fax: (+44) 1223-336-033; or deposit@ccdc.cam.ac.uk).

Received: August 10, 2004
Published online: November 18, 2004

